The development of seismic reflection sandbox modeling

Donald H. Sherlock and Brian J. Evans

ABSTRACT

Analog sandbox models provide cheap, concise data and allow the evolution of geological structures to be observed under controlled laboratory conditions. Seismic physical modeling is used to study the effects of seismic wave propagation in isotropic and anisotropic media, and to improve methods of data acquisition, processing, and interpretation. By combining these two independent modeling techniques, the potential exists to expand the benefits of each method. For seismic physical modeling, the main advantages are that the seismic data collected from these models contain natural variations that cannot be built into conventional solid models, which are machined with predetermined structures. In addition, the cost and construction time to build these models is significantly reduced. For sandbox modeling, the ability to record three-dimensional (3-D) seismic images before the model is manually sectioned for conventional two-dimensional (2-D) structural interpretation allows far more detailed study of subtle 3-D structures than previously possible.

In the past other workers have attempted to use unconsolidated sands for seismic physical models, but these attempts have been unsuccessful because of the lack of control or understanding of the natural variations that occur throughout the models. The aim of our research has been to overcome such problems and to develop techniques to alter the acoustic impedance of sand layers, thereby allowing the subsequent ultrasonic seismic recording of 3-D fault systems in sand analog geological models.

INTRODUCTION

Analog sandbox models are powerful tools in the study of structural processes in nature and have been used for many years to guide the structural interpretation of field and seismic data. Reflection seismology is the key method in mapping subsurface geology for petroleum exploration. Sandbox models, however, have not previously been used to test the correspondence of seismic images of geological structures with true geological sections.

The collection of scaled seismic data from physical models, known as "seismic physical modeling," has two great advantages

Manuscript received March 22, 1999; revised manuscript received October 3, 2000; final acceptance November 9, 2001.

AUTHORS

DONALD H. SHERLOCK ~ *Department of Exploration Geophysics, Curtin University of Technology, P. O. Box U1987, Perth, 6845, Western Australia; don.sherlock@per.dpr.csiro.au*

Don Sherlock graduated with a B.Sc. (hons) degree in geology from the University of Western Australia in 1995 and subsequently completed a Ph.D. in geophysics from Curtin University of Technology in Perth, Australia, in 1999. He is currently a research fellow in geophysics with CSIRO Petroleum in Perth, where he is collaborating with reservoir engineers and geophysicists from Curtin University to develop a physical modeling facility for seismic monitoring of hydrocarbon reservoir production.

BRIAN J. EVANS ~ *Department of Exploration Geophysics, Curtin University of Technology, P. O. Box U1987, Perth, 6845, Western Australia; evans@geophy.curtin.edu.au*

Brian Evans is an associate professor at Curtin University of Technology. He graduated from Liverpool as an electrical engineer in 1969 and has since completed an M.Sc. degree and Ph.D. in geophysics at Curtin University. Brian has worked on seismic operations throughout the world as both a staff geophysicist and geophysical consultant and is the author of the Society of Exploration Geophysicists book *Seismic Data Acquisition in Exploration.* Since 1985, Brian has lectured at Curtin University and is responsible for establishing new research projects.

ACKNOWLEDGEMENTS

This study was made possible through the financial support of Petroleum Geo-Services.

over working with field data. It is orders of magnitude cheaper than performing field surveys, and the geology is known so its effects on wave propagation can be directly measured and understood. Prior to the research presented here, however, all seismic physical modeling has been performed using solid models comprising predetermined structures, which imposes constraints on the realism of the model. Sandbox modeling is a dynamic process, developing structures that form with all the idiosyncrasies of natural systems. Hence, the production of scaled seismic data from such models provides a new modeling concept in understanding three-dimensional (3-D) geology.

In the past, several problems have prevented the application of seismic imaging methods to sandbox models. The most significant of these are the high rate of energy attenuation of acoustic waves in unconsolidated sand and our lack of understanding or control of the natural variations in grain packing that occur in the models. This has limited our ability to study how ultrasonic reflections can be produced from layers within sandbox models that have similar acoustic properties.

The fundamental goal of the work presented here is to address some of the limitations and to move the technology forward by understanding how seismic reflections may be produced within sandbox models in a controlled and predictable manner. Our results show that recording a scaled 3-D seismic image over a simple sandbox model before it is manually sectioned for conventional two-dimensional (2-D) structural interpretation allows far more detailed study of subtle 3-D structures than previously possible.

STATE OF THE ART

Sandbox Modeling

Analog sandbox models have proved to be very powerful tools in the study of structural processes produced in nature, especially where the phenomena are poorly understood (Vendeville et al., 1987). Such models offer cheap, concise data and allow the evolution of structures to be observed, leading to a better interpretation of structural systems. The model builder can control the boundary conditions and then compare the results of modeling to natural geological examples, to either negate or substantiate possible mechanisms for the development of geological structures. Such models have guided the structural interpretation of field and seismic data for more than 60 years (Vendeville and Cobbold, 1988; McClay, 1989; Withjack et al., 1995). The results of the modeling can be directly compared with geological structures for improved conceptual visualization of the processes involved. This type of modeling is very difficult to simulate numerically.

Construction of Models

A conventional sandbox model is constructed by depositing alternating layers of dry sand consisting of contrasting colors onto a base. Each layer of sand is typically around 2 mm thick and represents a lithological layer within a sedimentary sequence. The layers are sprinkled on by hand as evenly as possible and are initially horizontal to simulate a sedimentary sequence prior to deformation. Depending on the style of model being built, the base may be solid with a predetermined structure, such as a footwall, built in to represent the basement underlying the sedimentary sequence (Withjack et al., 1995). Alternatively, the base may consist of a flexible rubber sheet (Harris et al., 1994) or silicone putty (Gartrell, 1997) to simulate the ductile lower crust.

Deformation of sandbox models is commonly performed by computer-controlled stepper motors operating at a fixed strain rate that is scaled to simulate deformation over geological time from tectonic forces, although there are also examples where gravity can be used to induce deformation (Gartrell, 1997). As faults are initiated in the models, more layers of sand are added to the depressions that form to simulate syn-deformational sedimentation and to prevent the structures from collapsing

Rheology and Scaling

Rheology describes the response of a material to an imposed stress in terms of its elasticity and plasticity. Sandbox models commonly focus on brittle deformation in the upper crust, using dry cohesionless sand grains; however, they can also incorporate materials such as silicone putty or honey, analogous to the ductile lower crust and upper mantle. For laboratory results to be considered true analogs of natural structures, it is important that the materials and tectonic processes are accurately scaled (Ramberg, 1967).

Horsfield (1977) showed that the rheological properties of moderately cohesive sediments, with frictional plastic behavior at the time of faulting, could be simulated with dry sand after scaling down by a factor of between 1:10,000 and 1:100,000. Dry sand has an angle of internal friction $\phi = 30–32°$, which is similar to that determined for brittle sedimentary rocks in the

upper continental crust (Bryerlee, 1978). This value can, however, vary significantly depending on the handling technique employed (Krantz, 1991) and, as we show, also has a significant effect on seismic transmission properties. The deformation process obeys the Mohr-Coulomb failure criterion for faulting, in accordance with deformation mechanisms in the brittle upper crust (Jaeger and Cook, 1979). The characteristics of granular material mean that faults develop as dilational shear zones (Mandle et al., 1977), and the width of these is governed by the size and packing distribution of the grains.

The very low cohesive strength of dry sand makes the models essentially strain-rate independent, and allows deformation experiments to be performed over a reasonable length of time. Millions of years of tectonic deformation in sedimentary rocks are commonly simulated in less than a day. Although the cohesion between the sand grains is very small (most authors refer to it as "negligible"), it may be important in models involving fault reactivation (Richard and Krantz, 1991).

Sectioning

The fundamental approach for the analysis of the structures formed in analog models is manual sectioning of the model with a knife after deformation has been taken to completion. The most common means of consolidating the sand sufficiently to prevent the model from collapsing when sectioned is to saturate it with a water and gelatin mix. This process provides enough cohesion between the sand grains to allow sections of the model to be cut and photographed for later analysis without affecting the internal structure.

Sections can be cut in any orientation, even horizontally, but are typically cut vertically in the prevailing dip direction to reveal as much information as possible. In this orientation fault throws are at their maximum, and features such as antithetic faults, rollovers, and block rotations are revealed. Typically, sections are cut as closely together as possible to enable the 3-D geometry to be inferred from the 2-D sections. Most authors cite section spacings of 10 mm; smaller spacings are very difficult to cut by hand. This equates to scaled dimensions of 100 m to 1 km between sections, which is sometimes barely adequate to map the structure in three dimensions if the model contains complex faulting. Nevertheless, having multiple sections from the one geological setting is a luxury unavailable in the field and is a fundamental aspect of sandbox model analysis that makes it so powerful.

Surface Expression

Time-lapse photography is commonly used to record progressive stages of deformation as the model is being run. In most cases there is only limited information to be gained from this because it can record only the surface expression of the model. Syndeformational layers of sand are commonly added to the model at progressive stages, covering up the faults visible on the surface. The use of lighting at low angles to the surface, however, highlights any visible faults, and photographs of this aid in establishing the order that faults are initiated within the model. Although most modeling experiments are analyzed from section views, Higgins and Harris (1997) provided an example where a plan-view approach was used as the basis for the structural interpretation.

Three-Dimensional Computer Visualization

Three-dimensional seismic data are probably the oil industry's most significant technological advance in recent times. Interpretation of these data has been influenced by the analysis of analog models. Such models, however, have been analyzed almost entirely by traditional 2-D methods employing mostly cross sections, which commonly makes it impossible to understand the full 3-D geometry of complex models. Computer visualization software enables serial cross sections from a sandbox model to be digitized, interpolated, and rendered in three dimensions to aid in visualizing structurally complex geology. This technology has been used to great effect with salt-related analog models by Guglielmo et al. (1997). This is purely a visualization tool and does not provide any information that is not already available from the cross sections of the model. To visualize more subtle structures that may exist between each section, finer spatial sampling is required, which is one of the biggest potential benefits of developing the seismic imaging techniques described in this article.

Computerized X-ray Tomography

A recent innovation in imaging structures within sandbox models has been the adaptation of computerized x-ray tomography, or CT scans, for use with dry granular media. Manual sectioning of sandbox models means that the model is destroyed and only one orientation of sections can be made. CT scans have the advantage of being nondestructive, and, therefore, they allow sections to be imaged in several orientations. Another key benefit of this technique is that it allows the evolution of structures to be observed at progressive

stages of deformation. The CT technique was originally developed for medical imaging (Hounsfield, 1973). It was first adapted for use in geology to analyze rock properties and fractures in core samples (Vinegar, 1986; Raynaud et al., 1989). Its use in analyzing analog sandbox models was pioneered by Shell Oil Company laboratories (Mandl, 1988).

Computerized tomography is based on a set of attenuation profiles recorded from an x-ray beam. Absorption of x-radiation by any substance depends on its bulk density and atomic weight. The lower the density of the material, the more transparent it is to x-rays. If the materials used are relatively homogeneous, the resultant attenuation is roughly proportional to the local density (Desrues et al., 1996). Faults develop in granular materials as dilational zones and can result in a density contrast of around 30% (Colletta et al., 1991), and so they show up as areas of lower attenuation in the CT scan. Old faults that die out tend to recover their initial density, and so it is possible to visualize the fault chronology and emphasize out-of-sequence mechanisms.

Recording a successful CT image from a sandbox model is far from simple. The images contain considerable noise that is a result of density variations that inevitably occur from the nonuniform sorting of the sand (Mahmood, 1996). We show that this is a problem that also affects the seismic response in sandbox models.

Seismic Physical Modeling

The collection of scaled seismic data from physical models, known as "seismic physical modeling," has two great advantages over working with field data. It is orders of magnitude cheaper than performing field surveys, and the geology is known so its effects on wave propagation can be directly measured and understood. Such models, however, incorporate several simplifications and are restricted in their complexity.

Once a model has been built, ultrasonic transducers are used to record 2-D and 3-D seismic data under computer control in a known x, y, and z coordinate system. This capability offers great potential as a scientific tool to understand the seismic expression of various structural styles, and offers insight into future methods of 2-D and 3-D seismic acquisition and processing for improved target mapping. In 1991, a physical modeling system was constructed at Curtin University in Perth, Australia, where it is being used for studying the 3-D effects of seismic wave propagation in isotropic and anisotropic media.

Prior to the research presented here, all seismic physical modeling had to be performed using solid models, which are constructed with predetermined structures built into the model. This restriction imposed constraints on the realism or natural variation within the model. Sandbox modeling is a dynamic process, developing structures that form with all the idiosyncrasies of natural systems. Hence, the production of seismic profiles from such models would provide a new modeling concept in understanding 3-D geology. Developing the ability to apply such technology to cohesionless sand models also reduces the cost and time involved in construction of a physical model.

A major problem in the past that has prevented the application of seismic imaging methods to sandbox models has been the severe energy attenuation of acoustic waves as they travel through the sand matrices (Purnell, 1986). This is due to several factors such as energy loss caused by friction between grains in the unconsolidated matrix, an unrealistic ratio of grain size to seismic pulse wavelength, and problems of uneven pore-space distribution. In sandbox modeling, the sand is poured onto the model by hand, and therefore, it is impossible to achieve a completely uniform application of the sand grains. The heterogeneity of the grain packing arrays means that every sandbox model is unique. This is both an advantage and a disadvantage in that it adds a degree of realism to the model due to natural variation but also that the seismic response of each model is not consistently repeatable. This prompted seismic experiments on samples of grain mixes within consolidated matrices, such as silicon rubber (Purnell, 1986), and resins (Zhang et al., 1996), where grain distribution was more controllable. A fundamental goal of this work, however, was to overcome such problems and move the technology forward.

Scaling and Velocities for Seismic Physical Modeling

Most marine seismic data are within in the frequency range of 10 to 100 Hz. Therefore, a scale of between 1:10,000 and 1:100,000 could be modeled with a 1 MHz transducer, which was used for most of this research. When scaling physical models, the main rule that must be followed is that the ratio of geological feature size to wavelength must be the same in both field and model. The larger end of this range (1:10,000) was chosen for the sandbox models presented here to minimize problems associated with the grain size to wavelength ratio. A typical model area of 300 $\times$ 200

mm and depth of around 100 mm represents field dimensions of 3 × 2 km and a depth of 1 km.

The quartz sand used in most of these models has a mean grain size of 200 μm and a maximum of 300 μm, which, although a good analog for sedimentary rocks in terms of its deformational behavior, is not ideal in terms of the seismic response. A grain size of 200 μm represents the equivalent of a 2 m diameter boulder, which is around one eighth of the seismic wavelength used in these experiments. Grains larger than this behave as individual reflectors and contribute to the significant amount of noise that occurs in these models from scattering of the signal. Therefore, larger grain sizes should not be used. Although the grain size to wavelength ratio cannot be scaled realistically, the individual grains are below the limit of the seismic resolution and, hence, do not change the seismic expression of the model structures. This is, however, a significant limitation if the goal is to relate the acoustic properties of individual layers measured at ultrasonic frequencies to the properties of similar unconsolidated sands measured in the field at seismic frequencies.

Finer grain sizes are desirable to reduce the degree of scattering, but this in turn creates other problems when saturating the models in preparation for the seismic surveys because of the reduced permeability. It is necessary to develop techniques that ensure that finer grained models can be fully saturated before they can be used successfully for seismic imaging. Methods under consideration to achieve this in future models are to saturate the models while in a vacuum chamber or to use wetting agents to reduce the air-water interfacial tension, which in turn allows the water to permeate into the smaller pores.

Many modeling materials have velocities much lower than true rock velocities, and because of this the time scale is commonly specified independently of the distance scale. Note that both the distance scale and time scales are, in a sense, arbitrary, because both the horizontal and vertical axes can be stretched or squeezed by resampling when displaying the seismic section.

Data Recording and Processing

The physical modeling system used for this research (Figure 1) comprises a personal computer (PC) driving an ultrasound pulser unit, using ultrasonic piezoelectric transducers for the source and receiver. Movement of the transducers is controlled in three dimensions by stepper motors that are driven by the PC in an x, y, and z coordinate system.

Once a model has been built using dry granular materials, it is saturated and placed in a large tank of water. Ultrasonic transducers are positioned over the model to simulate a marine environment, thereby recording acoustic waves. Any configuration of 2-D or 3-D seismic data can be collected under computer control. The data for the models in this article were collected at zero offset, using the same transducer for both source and receiver. Conventional surveys using variable offsets and common midpoint (CMP) stacking can also be performed, which is necessary to image the more complex structures that are found in typical sandbox models. To do so, however, presents further problems that are related to the particular type of high-energy transducer that is needed for sandbox models (Sherlock, 1999).

The output from the receiver is fed into a 12-bit analog-to-digital converter and then stored on disk or downloaded over the network directly onto an Exabyte magnetic tape in SEG-Y format. The volume of data collected is similar in size to that collected in the field. Hence a large disk and tape capacity is a prerequisite to recording, plus the requirement of processing data on fast computers.

Data processing is performed using interactive workstations networked to a Sun 1000E processor within the Department of Exploration Geophysics at Curtin University and uses the Landmark software PROMAX. Complex processing steps were not required because of the simple structure of the models presented here. For example, it was not necessary to include techniques to remove multiple reflections from the data because the source and water depth were designed such that all multiples would arrive at traveltimes later than the primary reflections of interest. More sophisticated processing sequences can, however, be easily implemented when required to better image more complex models as they are developed. The only processing applied to the recorded data for the display of the data and calculation of the reflection coefficients was a gain function to recover the amplitudes lost through spherical spreading of the source energy and absorption. Three-dimensional visualization is performed on a Silicon Graphics workstation and uses the Paradigm software VOXELGEO.

Seismic Reflection Theory

Conventional theory states that for a seismic reflection to result between two layers of rock there must be an acoustic impedance contrast. Acoustic impedance

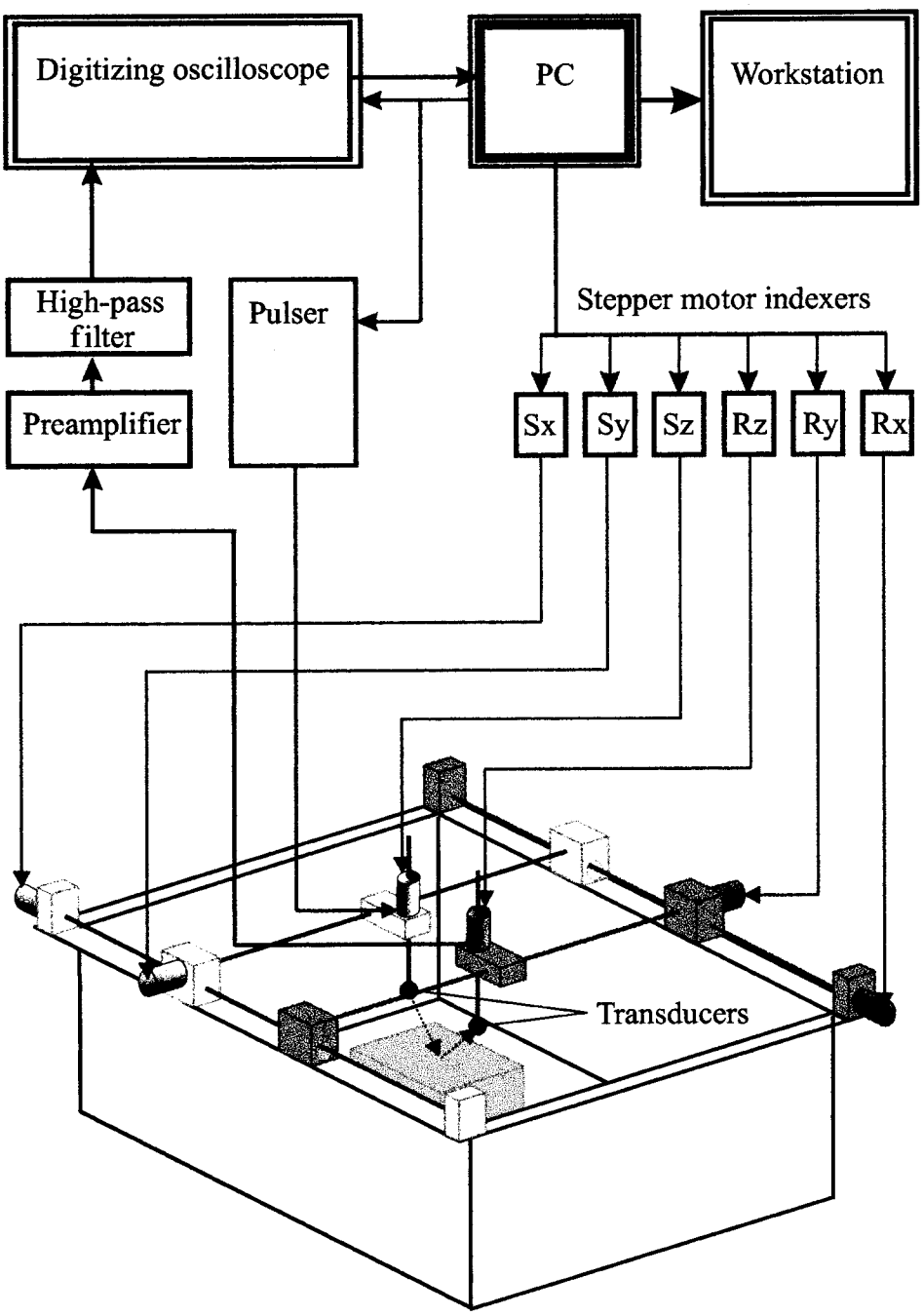

Figure 1. Schematic diagram of the components that make up the physical modeling system at Curtin University of Technology in Perth, Australia.

(Z) is defined as density (ρ) times velocity (V). Therefore, a seismic reflection should result whenever there is a change in rock density or velocity. The strength of the reflection, that is, the percentage of energy reflected, is dependent on the reflection coefficient (R_c), which is defined by the formula

$$R^c = \frac{(Z_2 - Z_1)}{(Z_2 + Z_1)}$$

where Z_1 and Z_2 are the respective upper and lower layer acoustic impedances.

With consolidated rocks, velocity is mainly influenced by density (which is dependent on mineralogy, porosity, and fluid type), degree of cementation, pressure, and temperature. The relationship of these factors to velocity is described by the Biot-Gassman equation (Biot, 1956a, b). In the case of unconsolidated sediments, however, the influence of these factors is less clear. Density no longer plays a significant role, and

the major factors become pressure, temperature, and frame rigidity. Bell and Shirley (1980) showed that the type of loose material makes no difference to the compressional wave (P-wave) velocity. Talwani et al. (1973) showed that loose sediments exhibit hysteresis, that is, the velocity change with increasing pressure is reversible whereas the porosity change is not. This demonstrates that the velocity is not dependent on porosity.

At room temperature and pressure, the major influence on loose sediment velocity is the rigidity of the sediment frame (matrix) and fluid type. For the purpose of this article, the fluid used is always fresh water and so can be neglected. The rigidity of the sediment matrix can be expressed in terms of the bulk modulus (K), which is defined as

$$K = \frac{\rho V^2}{1 + Q}$$

where V is the P-wave velocity, ρ is the density, and Q is the rock quality factor. For materials of similar density and velocity, the bulk modulus is approximately inversely proportional to Q, which can be thought of as the ability of the sediment to transmit seismic energy. Q is also related to the attenuation coefficient (α), which is the exponential decay constant of the amplitude of a plane wave traveling in a homogeneous medium. They are related as follows:

$$\frac{1}{Q} = \frac{\alpha V}{\rho f}$$

where f is the dominant frequency. The grain packing and degree of consolidation govern Q. In unconsolidated sands the packing is dependent on grain shape and sorting.

EXPERIMENTS

Sand Velocities

When considering measured velocities of unconsolidated sands in the laboratory it is important to keep in mind several factors:

1. The low total pressure (atmospheric) and zero effective pressure (confining pressure minus pore pressure) mean that the rate of energy absorption through friction between the grains is extremely high. This requires that the length of the sand sample used for velocity tests be kept small to allow a transmitted pulse to be recorded between ultrasonic transducers, which subsequently results in high measurement errors.
2. A fraction of a percent of gas is known to have significant effects on velocity (Domenico, 1976), and it is difficult to ensure that all of the air has been expelled from the samples.
3. Velocities are calculated from first-arrival traveltimes, and it is assumed that the ray path traveled is the shortest direct path, but this is not necessarily the case (Wyllie et al., 1958). The direct path may in fact be slower than the waves through the fluid in the matrix, or be attenuated by the transitions between fluid to grain, to the point of being imperceptible. The fastest waves may be those that travel only in the sand grains and follow a longer zig-zag path through sand grain contacts.
4. The sands used by different researchers may have similar average grain sizes, but they are not the same samples. Subtle variations in sorting and grain shape make little difference to the porosity and density but have large effects on the frame rigidity and subsequently the velocity.
5. The effects of velocity dispersion, whereby different frequencies travel at different velocities are not fully understood. In most cases with pulse measurements the first arrival is assumed to be the dominant frequency or the highest frequency. Liu and Nur (1996), however, suggested that the first break is the lowest frequency.
6. Vibration applied to the loose sand packages makes a significant difference to the packing of the grains. This is illustrated by observing a sand velocity of 1600 ms^{-1} before vibration, compared with 1730 ms^{-1} measured from the same sample after vibration, which is consistent with measurement by many researchers, both in situ and in the laboratory.

For these reasons, estimated errors for velocity measurements are commonly on the order of 100 ms^{-1}, depending on the frequency used. Chotiros (1995) estimated an error of ± 300 ms^{-1} below 15 kHz. We recorded velocities of individual sand samples used in the models (all without vibration) using acoustic pulse transmission measurements (1 MHz), and all samples were within the range 1600 to 1700 ms^{-1}, varying less than the estimated measurement error. These measurements are considered accurate enough to demonstrate that the reflections produced in the

pure sand models are not primarily a result of the velocity contrast between different layers. Velocities as high as 2000 ms^{-1} were recorded for mixtures of sand and clay (kaolin) powder. The sands tested in this article were assumed to have no gas content, and attempts were made to ensure this. Nevertheless, it is not known for certain that all of the air was expelled, particularly with the less permeable sand and clay mixtures.

MODELS

The standard sand used as a basis for these models comprised subrounded pure quartz grains. This sand is poor to moderately sorted with a maximum grain size of 300 μm and an average around 200 μm. The porosity was measured by weighing a known volume of the sand under room-dry and fully saturated conditions. The standard sand has a porosity of 35% and a saturated density of 2.05 g cm^{-3}. Other variations of sands used were made from sieved fractions of the standard sand. There was little variation in the measured porosities and densities except when a very narrow range of grain sizes was used, in which cases the porosity was as high as 38%.

All of the models were constructed in the same manner, with the only variations being the particular sand used in each of two layers. The first sand (lower layer) was poured into a container with dimensions approximately 200 × 100 mm and a depth of 50 mm. At a depth of 20 mm the sand was graded flat to produce a horizontal surface. The second sand (upper layer) was then carefully sprinkled on top so that the surface of the first sand was not disturbed. The models were then saturated with water and placed in a large water tank in preparation for the seismic experiments. A 2-D zero offset seismic line was then recorded over each of the models using a 1 MHz piezoelectric transducer as both the source and receiver. A scale factor of 1:10,000 was applied so that the recorded data could then be analyzed with conventional seismic data processing software.

Reflection coefficients were estimated from the amplitudes recorded at the layer interface relative to the surface. The rate of energy attenuation within the sands has not been precisely determined at this stage, and therefore, it is likely that significant errors exist in the estimated reflection coefficients. In the following examples, the resulting reflections were very strong and the observed amplitudes indicate reflection coefficients around 0.2, which is at least 10 times greater than that predicted from the calculated acoustic impedances.

Example 1: Change in Grain Size

Results

The first example comprises the standard sand for the top layer whereas the sand for the bottom layer was sieved so that its average gain size was halved to 100 μm. The porosity of this lower sand was reduced to 30%, and the density was subsequently raised to around 2.1 g cm^{-3}. The measured velocity of this sand did not change perceptibly, and the estimated reflection coefficient was 0.02. Because the depth to the layer interface is the same in all of the examples (20 mm), the velocity of the overlying sand could be easily checked from the two-way traveltimes between the model surface and the first reflection and was consistently between 1600 and 1700 ms^{-1}. Figure 2 shows the seismic section recorded over this model; the observed reflection coefficient was at least 0.2, which is an order of magnitude greater than that predicted from the acoustic impedances.

Interpretation

This first example shows that it is possible to produce a strong reflection between unconsolidated sediments with nearly identical density and velocity, using only a variation in grain size. The reflection coefficient is at least an order of magnitude larger than that predicted from the calculated acoustic impedance contrast. We suggest that the reflection is not a result of a change of characteristics between the different sands used, but instead a consequence of the interaction of the two mixtures at the layer interface. McGeary (1961) showed with experiments on the mechanical packing of spheres how the packing of grains altered depending on the sorting of grain sizes. From these results it is concluded that the porosity at the interface of the two sand layers may be as low as 10%. A precise estimate is not possible because the actual figure is strongly dependent on the amount of settling that occurs, which arranges the grains into the most stable packing order. Although the porosity change does not directly alter the acoustic properties, it is the effect on the rigidity of the grain packing that produces the contrast.

The strong reflection is interpreted to be a result of the change in grain packing that occurs at the interface between the two layers. This effectively creates a third layer of around one grain thickness, where the

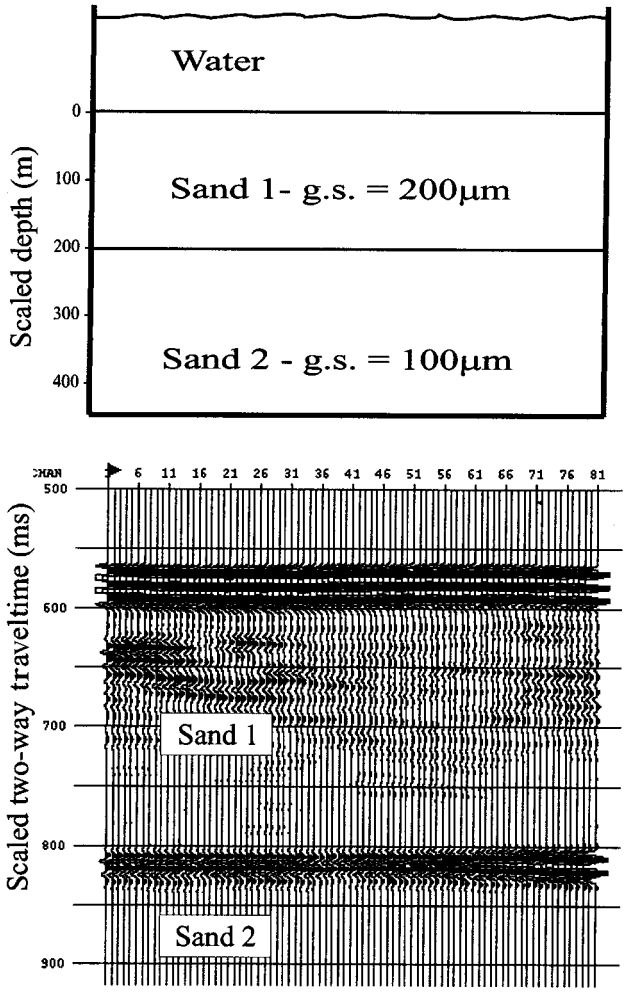

Figure 2. Schematic diagram and scaled seismic section of a two-layer sand model where the strong reflection from the layer interface is caused by a contrast in grain size between layers. The data has been scaled by a factor of 1:10,000; g.s. = grain size.

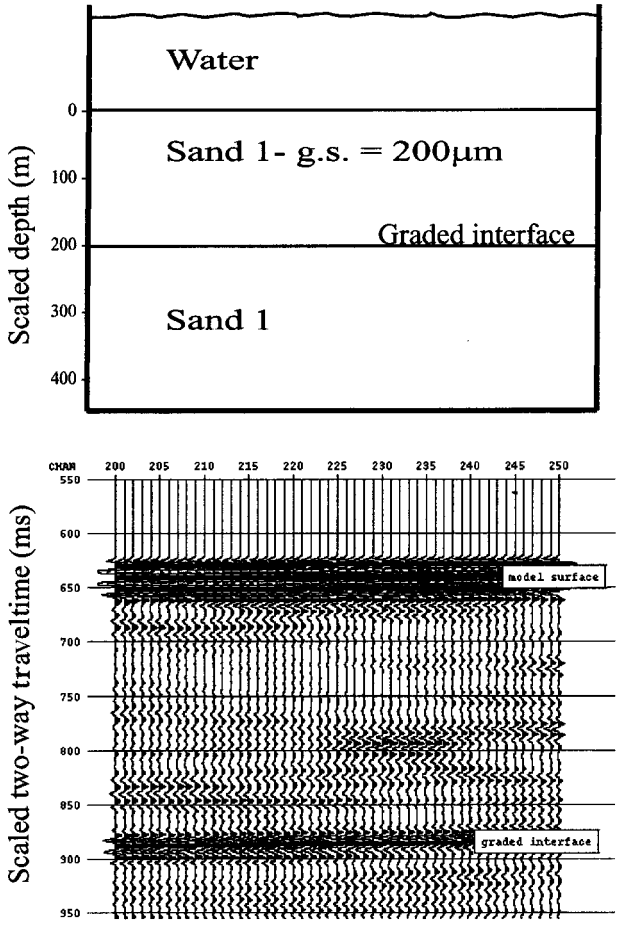

Figure 3. Schematic diagram and scaled seismic section of a two-layer sand model where the same sand is used for both layers. The reflection from the interface is caused by the change in grain packing that occurs from the action of grading a flat surface on the lower layer. g.s. = grain size.

packing is more dense and subsequently the porosity is reduced and the frame rigidity is increased. This third layer is analogous to a thin bed in the real world, such as a low-porosity shale lens between two high-porosity sands. Although this layer is too thin to be resolved as an individual layer in the seismic data, the sharp change in acoustic properties produces a reflection. The following experiments show that either a change in average grain size or simply a change in grain sorting can produce such a reflection.

Example 2: Same Grain Size, Change in Packing

Results

A clearer illustration of the significance of localized changes in grain packing is shown in Figure 3, which shows a reflection from an interface where the same sand was used for both layers of the model. As with the other models, the top surface of the lower sand was graded to be horizontal before the upper sand was added, but in this case the same sand was used again for the upper layer. The resulting reflection coefficient is approximately 0.1.

Interpretation

In this case there is no contrast in grain size between the two layers that can create the third layer that has been suggested as the reason for the strong reflection in the first example. Although the reflection coefficient of around 0.1 is half that of the first example, it is still a very strong reflection that must have been generated by a contrast in properties at the layer interface.

Our interpretation of this result is that it must have been caused by the action of grading the flat surface into the lower sand layer before the upper layer was added. This flat surface was created artificially within the models by dragging a board over the surface of the sand at a fixed level. Although this action is not analogous to any geological process, it was performed to ensure that the interface was perfectly horizontal and at the same depth within every model. In this way, it is possible to accurately compare differences in the interval velocity of each model, and it allows the interface to be interpreted unambiguously in models with very subtle reflections or low signal-to-noise ratios. We suggest that the process of grading the flat horizon causes localized changes in the grain packing and sorting at the interface between the two sands. As the board is dragged along the sand surface the smaller grains fall into the cavities of the larger grains, resulting in a more tightly packed grain matrix at the interface. Results of repeated experiments in which the intensity of this grading process was varied support this conclusion.

Example 3: Multilayer Reflections from Sand and Clay Mixtures

Results

Horizontal layers comprising mixtures of sand and clay (kaolin) were shown to produce strong reflections within models of pure sand. Kaolin appears to stiffen the contacts between the quartz grains (Han et al., 1986). This has the effect of raising the acoustic velocity by raising the bulk modulus of the grain matrix. Limitations on the energy output of the transducers and the high rate of absorption through the uncemented grains make it very difficult to image multiple layers at this stage. Various combinations of mixtures at different depths were tested in an attempt to achieve the best balance of reflected and transmitted energy, thereby allowing as many layers to be imaged as possible. Figure 4 shows a 2-D seismic profile recorded over a model containing four reflecting horizons plus the model surface. The depth to the first layer is 20 mm (200 m scaled), and each subsequent depth interval is progressively smaller to ensure that any multiple reflections that are generated between layers arrive after the last primary reflection of interest. The third and fourth horizons are separated by just 2 mm (20 m scaled) and are difficult to resolve because of the resonant nature of the seismic signal.

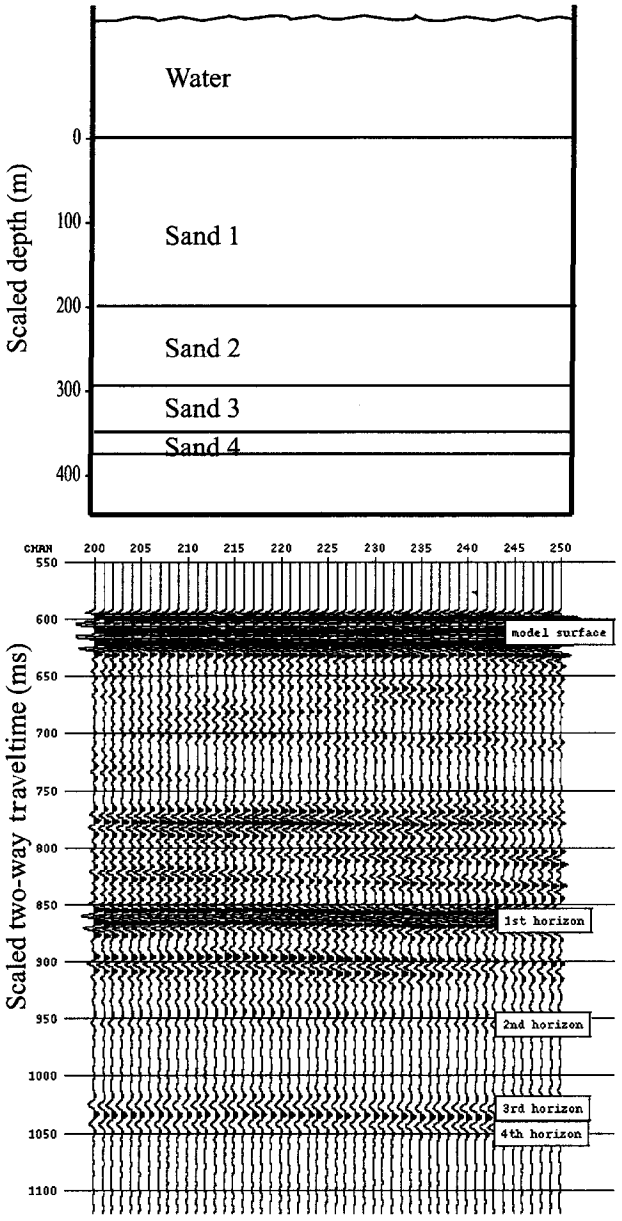

Figure 4. Schematic diagram and scaled seismic section from a sandbox model containing four layers of different sand and clay mixtures.

Interpretation

Manually sprinkling the sand into the model container results in a natural sorting of the grains. This is analogous to the way fining-upward sequences are deposited in fluvial systems, with the larger grains coming to rest first and finer grains depositing farther down stream. The result is that each single body of sand deposited within a particular layer in the model is effectively a fining-upward sequence, which has major implications on the grain packing within the layer. This effect in a

container is sufficiently profound to result in low-amplitude reflections within each of the sand layers, which were initially assumed to be homogeneous.

Evidence that these reflections are a result of the natural segregation of the grains as they are deposited is provided by the fact that the greatest effect occurs when the sand is poorly sorted. Such reflections can be clearly seen between the main horizon reflections in Figure 4. This effect is reduced when using well-sorted sands, such as the lower sand in Figure 3, where there is less variation in grain size and subsequently less sorting possible.

Example 4: Reflections from Natural Variations in Sorting

The natural sorting of the sand grains illustrated in the previous example can be exploited to produce a strong coherent stratigraphic-style reflection throughout a sandbox model. Figure 5 shows an interpretation of three horizons from a 3-D seismic volume recorded over such a model. The 3-D survey was recorded with a zero-offset configuration whereby the same transducer is used for both the source and receiver and the seismic waves are transmitted and reflected vertically. The upper and lower horizons are reflections from layer interfaces in the model where there is a contrast in grain sizes. The middle horizon has been interpreted from a reflection that has been generated within a single body of sand that exists between the upper and lower horizons. This reflection was generated intentionally by exaggerating the effects demonstrated in the previous examples. The middle sand was deposited as two separate scoops of sand taken from the same bucket. Each scoop was slowly sprinkled into the model container to allow the natural sorting of grains to occur. This effect could be seen with the naked eye as the larger grains tended to rise to the top of the scoop and fall into the container first, leaving a greater proportion of the finer grained fraction to fall in last. This created a natural fining-upward sequence within the layer, resulting in a contrast in packing at the interface with the following scoop of sand.

Wedge Model

An example of the resolution possible from seismic sandbox modeling is shown in Figure 6. The model comprises a three-layer case where the top sand layer lies on an angular unconformity so that the middle sand layer forms a wedge that pinches out at the unconformity. The seismic display is a close-up of this pinch-out, with a field of view approximately 10 mm^2 (100 m^2 in scaled terms). The unconformity is clearly imaged, and tuning effects can be seen as the middle layer pinches out. These tuning effects are a result of interference between the reflections from the upper and lower interfaces of the wedge. In addition, a much subtler depositional feature of the sand onlapping onto the unconformity is also imaged.

Gas/Fluid Contacts

The use of sands in seismic physical modeling allows different fluids to be incorporated for the first time, providing an analog of hydrocarbon reservoirs. Figure 7 shows the seismic data recorded over a sandbox model where a pocket of air has been trapped under an impermeable shale anticline. A flat spot can be clearly seen at the contact between the trapped air and the underlying water. Similar experiments are currently being developed with models that contain more transitional and subtle contacts between oil and water.

Rift Graben

The aim of the next model is to demonstrate the ability to record a seismic image from a more conventional style of sandbox model, where the structures are created by actively deforming the model, rather than contrived as in the previous examples. Figure 8 shows the apparatus used to produce a simple rift graben. A plastic sheet underlies half of the sand in the container and is attached to a moveable end wall. As the wall was slowly pulled away, a rift developed in the middle, which was continuously infilled to simulate synrift sedimentation and to prevent the structure from collapsing.

A 3-D seismic survey was performed by running 50 parallel 2-D profiles at spacings of 1 mm (10 m scaled). The reflecting horizon and faults were interpreted on a workstation and are displayed in a 3-D volume form in Figure 9. The image clearly defines a rift graben bounded by normal faults. The position of these faults varies laterally along the strike of the graben, which is also seen on time slices of the model. Two small raised blocks are visible on the base of the graben, which trend orthogonally to the strike of the rift, along with a small displacement fault, which can be seen on the upper reflecting horizon to the west.

After the seismic data were recorded, the model was physically sectioned with a knife at spacings of 10 mm, corresponding to a section along every tenth

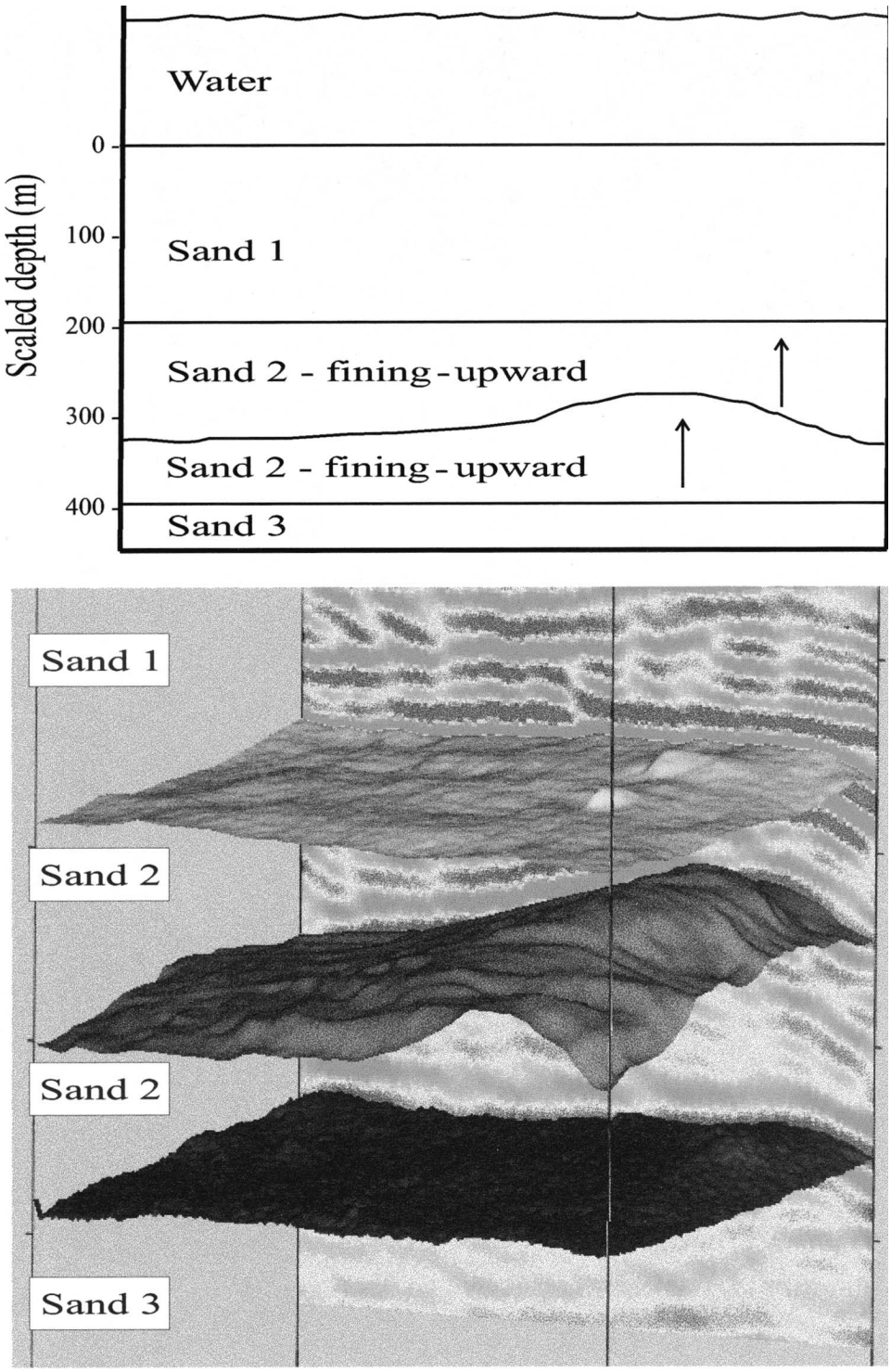

Figure 5. Schematic diagram and 3-D visualization of three reflecting horizons within a sandbox model. The reflections for the upper and lower horizons are generated by a contrast in grain size between layers. The middle reflection is a result of natural sorting of the sands as they are deposited into the model.

seismic line. The model sections reveal the gross form of the faults but are unable to resolve the finer details of the model that are seen in the seismic interpretation. Without the seismic data, these subtle details would remain undetected, which illustrates the improvement in resolution that is possible using this new technology.

DISCUSSION

The effects of the small-scale heterogeneities within the sandbox model shown do not arise in other studies of velocities and attenuation within sand, because they are invariably experiments involving acoustic transmission,

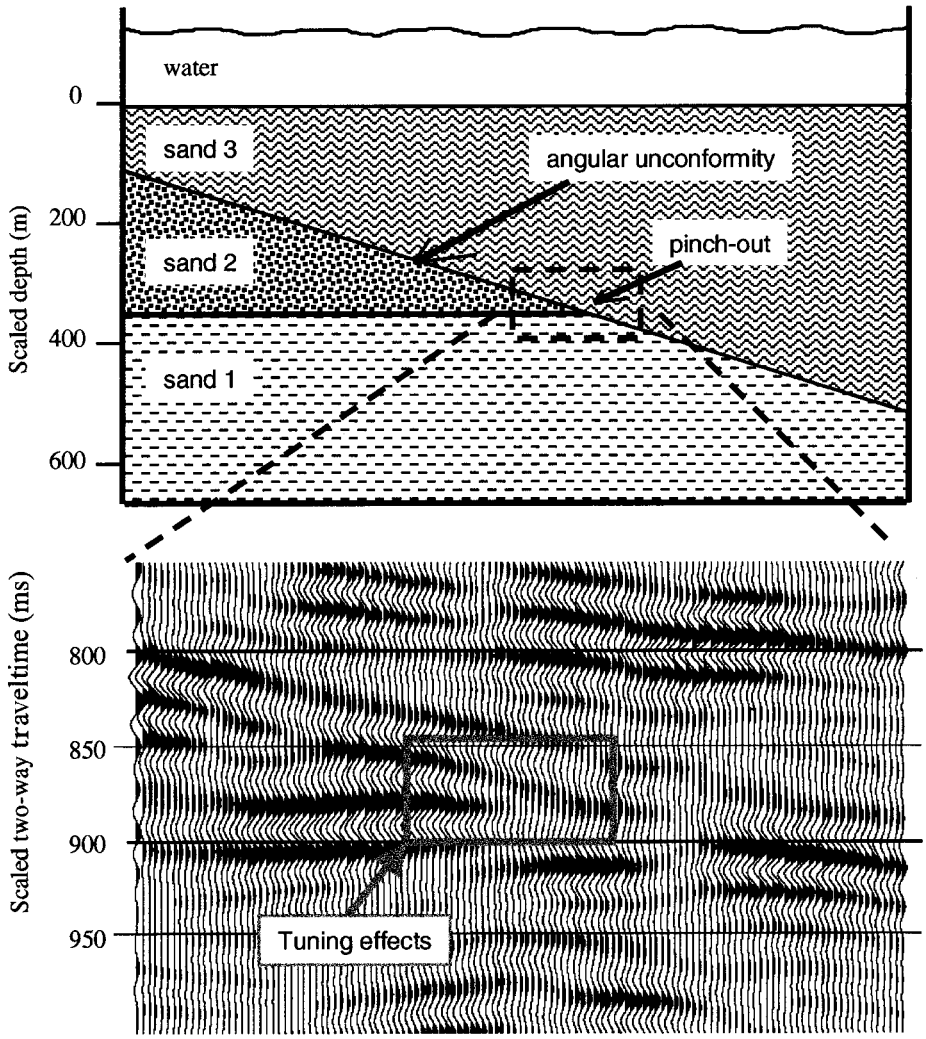

Figure 6. Schematic diagram and scaled seismic section of a three-layer sandbox model containing an unconformity. The seismic display is a close-up of the pinch-out in the model. Note the tuning effects of the waveform as the middle sand layer gets thinner and also the seismic expression of the top sand layer onlapping the unconformity.

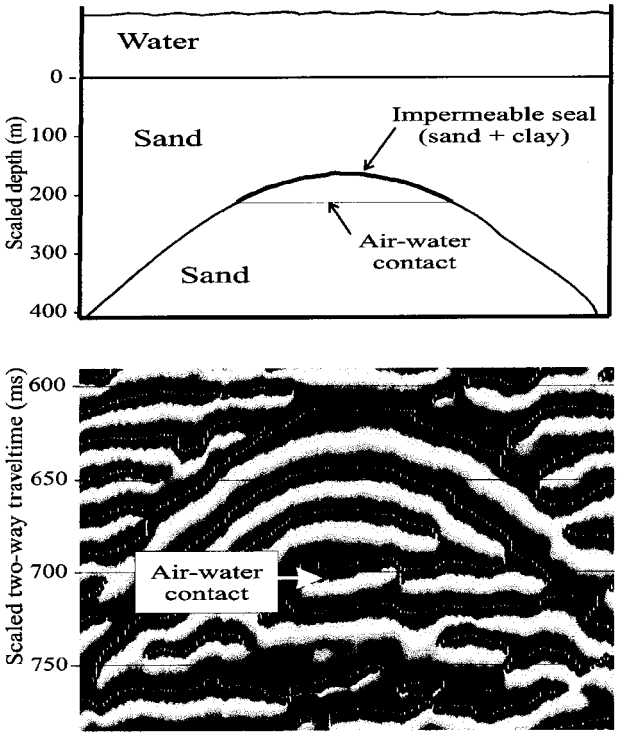

Figure 7. Schematic diagram and scaled seismic display of an anticline sand model. A pocket of air is trapped under an impermeable seal, creating a flat spot at the air-water contact within the model.

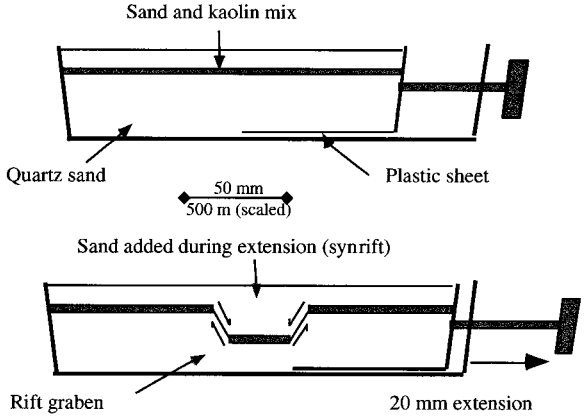

Figure 8. Schematic diagram of the apparatus used to generate a simple rift structure within a sandbox model. As the right end wall is extended, extra sand is added to the graben as it forms, simulating synrift sedimentation and preventing the structure from collapsing.

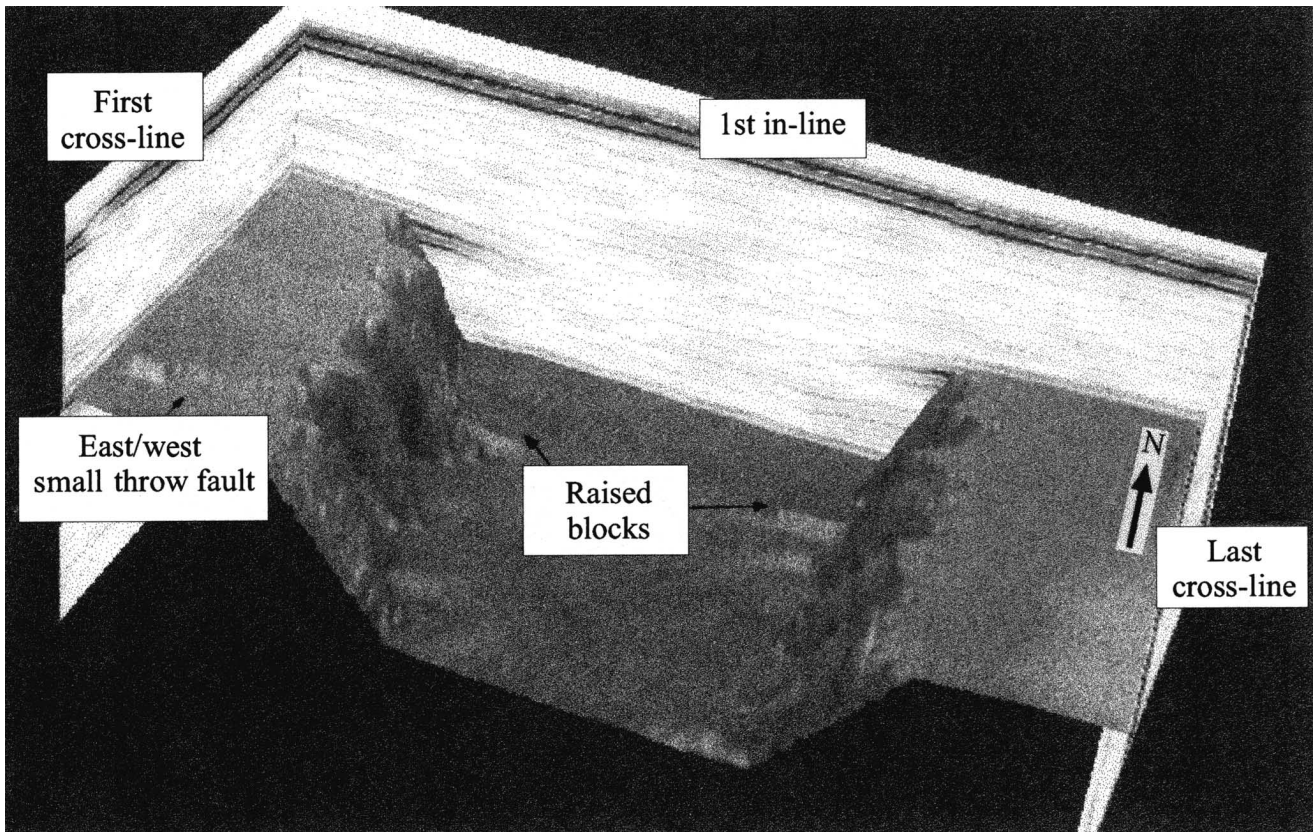

Figure 9. A 3-D interpretation of the sand and clay (shale) horizon reflection. Detailed features such as the raised blocks in the graben and the small throw fault to the west were not apparent in the manually cut sections of the model.

not reflection. The heterogeneities exist within any one sample, and therefore, the effects on velocity and attenuation are averaged over the length of the sample that the transmission is being recorded through. Calculations of parameters such as the bulk modulus from these results do not indicate how the modulus may vary at any one point within the sample. With the experiments presented here, however, any reflections recorded must be a result of a change within the model, which can only be from localized variations in grain packing. The reflections are analogous to seismic stratigraphic effects and complicate the assumptions on attenuation because, although the energy is being reflected and not absorbed, it has the similar effect of reducing the amount of energy that is transmitted through to the layer boundary. These stratigraphic reflections are highly sensitive to the manner in which the sand is poured into the containers.

This technology, although still in its infancy, is applicable to all forms of sandbox models. The high degree of resolution demonstrated in these simple models suggests this technique could potentially help with the interpretation of more complex models that prove difficult to interpret from sections alone. New forms of sandbox models that incorporate different fluids can also be considered for modeling hydrocarbon reservoirs. Other issues that are currently challenges for the seismic industry, such as subsalt imaging or time-lapse seismic could also be examined within a controlled laboratory environment using this technology.

CONCLUSIONS

Seismic physical modeling experiments with unconsolidated sand packages have shown that seismic reflections can result at boundaries between layers of equal density and velocity. Conventional theory suggests that a contrast in acoustic impedance between adjacent layers be required to produce such a reflection. We suggest that, although two different sand layers may have similar or identical acoustic impedances, there is effectively a third layer at the interface itself where the combination of the sands produces the required acoustic impedance contrast.

Developing techniques to combine the methods of analog sandbox modeling and seismic physical modeling have shown the potential to expand the benefits of each method. For seismic physical modeling, the ability to use sandbox models dramatically reduces the cost and time involved in construction of models while adding a degree of realism not previously possible. For sandbox modeling, the ability to record seismic images over them allows far more detailed interpretation of the structures.

Closer study of the seismic sections reveals that it is not only possible to accurately map the structure of the reflecting horizons in three dimensions, but that more subtle depositional features within each sand layer can also be imaged. This shows that as well as adapting these methods to the wide range of existing analog sandbox model varieties, there is the potential to develop new styles as well.

REFERENCES CITED

Bell, D. W., and D. J. Shirley, 1980, Temperature variation of the acoustical properties of laboratory sediments: Journal of the Acoustical Society of America, v. 68, p. 227–231.

Biot, M., 1956a, Theory of propagation of elastic waves in a fluid saturated porous solid: I–low frequency range: Journal of the Acoustical Society of America, v. 28, p. 168–178.

Biot, M., 1956b, Theory of propagation of elastic waves in a fluid saturated porous solid: II–high frequency range: Journal of the Acoustical Society of America, v. 28, p. 179–191.

Bryerlee, J., 1978, Friction of rocks: Pure and Applied Geophysics, v. 116, p. 615–626.

Chotiros, N. P., 1995, Biot model of sound propagation in water saturated sand: Journal of the Acoustical Society of America, v. 97, p. 199–214.

Colletta, B., J. Letouzey, R. Pinendo, J. F. Ballard, and P. Bale, 1991, Computerized x-ray tomography analysis of sandbox models: examples of thin-skinned thrust systems: Geology, v. 19, p. 1063–1067.

Desrues, J., R. Chambon, M. Mokni, and F. Mazerolle, 1996, Void ratio evolution inside shear bands in triaxial sand specimens studied by computed tomography: Geotechnique, v. 46, p. 529–546.

Domenico, S. N., 1976, Effect of brine-gas mixture on velocity in an unconsolidated sand reservoir: Geophysics, v. 41, p. 882–894.

Gartrell, A. P., 1997, Evolution of rift basins and low-angle detachments in multilayer analog models: Geology, v. 25, p. 615–618.

Guglielmo, G. J., M. P. A. Jackson, and B. Vendeville, 1997, Three-dimensional visualization of salt walls and associated fault systems: AAPG Bulletin, v. 81, p. 46–61.

Han, D., A. Nur, and D. Morgan, 1986, Effects of porosity and clay content on wave velocities in sandstones: Geophysics, v. 51, p. 2093–2107

Harris, L. B., R. I. Higgins, M. C. Dentith, and M. F. Middleton, 1994, Transtensional analogue modelling applied to the Perth basin, Western Australia, *in* The sedimentary basins of Western Australia: Proceedings of the Petroleum Exploration Society of Australia, p. 801–809.

Higgins, R. I., and L. B. Harris, 1997, The effect of cover composition on extensional faulting above re-activated basement faults: results from analogue modelling: Journal of Structural Geology, v. 19, p. 89–98.

Horsfield, W. T., 1977, An experimental approach to basement controlled faulting: Geologie en Mijnbouw, v. 56, p. 363–370.

Hounsfield, G. N., 1973, Computerized transverse axial scanning (tomography): British Journal of Radiology, v. 46, p. 1016–1022.

Jaeger, J. C., and N. G. W. Cook, 1979, Fundamental rock mechanics: London, Cambridge University Press, 593 p.

Krantz, R. W., 1991, Measurement of friction coefficients and cohesion for faulting and fault reactivation in laboratory models using sand and sand mixtures: Tectonophysics, v. 188, p. 203–207.

Liu, X., and A. Nur, 1996, A new experimental method for studying velocity dispersion in rocks (abs.): Society of Exploration Geophysicists 66th International Meeting, Expanded Abstracts, v. 2, p. 1683–1686.

Mahmood, T., 1996, ATLAS 3D analogue modelling of extensional fault systems plus field applications: Ph.D. thesis, University of Adelaide, Australia, 187 p.

Mandl, G., 1988, Mechanics of tectonic faulting: models and basic concepts: Amsterdam, Elsevier, 407 p.

Mandle, G., L. N. J. D. Jong, and A. Maltha, 1977, Shear zones in granular material: Rock Mechanics, v. 9, p. 95–144.

McClay, K., 1989, Analogue models of inversion tectonics, *in* M. Cooper and G. D. Williams, eds., Inversion tectonics: London, Geological Society, p. 41–59.

McGeary, R. K., 1961, Mechanical packing of spherical particles: Journal of the American Ceramics Society, v. 44, p. 513–522.

Purnell, G. W., 1986, Observations of wave velocity and attenuation in two phase media: Geophysics, v. 51, p. 2193–2199.

Ramberg, H., 1967, Gravity, deformation and the Earth's crust: New York, Academic Press, 452 p.

Raynaud, S., D. Fabre, F. Mazerolle, Y. Geraud, and H. J. Latiere, 1989, Analysis of the internal structure of rocks and characterization of mechanical deformation by a non-destructive method: x-ray tomodensitometry: Tectonophysics, v. 159, p. 149–159.

Richard, P., and R. W. Krantz, 1991, Experiments on fault reactivation in strike-slip mode: Tectonophysics, v. 188, p. 117–131.

Sherlock, D. H., 1999, Seismic imaging of sandbox models: Ph.D. thesis, Curtin University of Technology, Perth, Western Australia, 323 p.

Talwani, P., A. Nur, and R. L. Kovak, 1973, Compressional and shear wave velocities in granular materials to 2.5 kilobars: Journal of Geophysical Research, v. 78, p. 6899–6909.

Vendeville, B., and P. R. Cobbold, 1988, How normal faulting and sedimentation interact to produce listric fault profiles and stratigraphic wedges: Journal of Structural Geology, v. 10, p. 649–659.

Vendeville, B., P. R. Cobbold, P. Davy, J. P. Broun, and P. Choukroune, 1987, Physical models of extensional tectonics at various scales, *in* M. P. Coward, J. F. Dewey, and P. L. Hancock, eds., Continental extensional tectonics: Geological Society of London Special Publication, v. 28, p. 97–107.

Vinegar, H. J., 1986, X-ray CT and NMR imaging of rocks: Journal of Petroleum Technology, v. 38, p. 257–259.

Withjack, M. O., Q. T. Islam, and P. R. LaPointe, 1995, Normal faults and their hanging-wall deformation: an experimental study: AAPG Bulletin, v. 79, p. 1–18.

Wyllie, M. R. J., A. R. Gregory, and G. H. F. Gardner, 1958, An experimental investigation of factors affecting elastic wave velocities in porous media: Geophysics, v. 23, p. 459–493.

Zhang, M., D. A. Ebrom, J. A. McDonald, and R. H. Tatham, 1996, Comparison of experimental velocity measurements with theoretical results in a solid-solid composite material: Geophysics, v. 61, p. 1429–1435.